

# DOSIMETRY AND FIRST RADIOPHYSICAL ASSAY OF MULTI-Gy, MULTI-MEV TNSA PROTON BEAM WITH ULTRAHIGH DOSE-RATE

D. Giove, INFN-LASA, Segrate, Italy

F. Baffigi, F. Brandi, L. Fulgentini, L.A. Gizzi<sup>1</sup>,

P. Koester, L. Labate<sup>1</sup>, D. Palla, M. Salvadori, ILIL, CNR-INO, Pisa, Italy

R. Catalano, G.A.P. Cirrone<sup>2</sup>, M. Guarnera, G. Milluzzo, G. Petringa, INFN-LNS, Catania, Italy

A. Fazzi<sup>3</sup>, Politecnico di Milano, Milano, Italy

M. G. Andreassi, A. Borghini, Istituto di Fisiologia Clinica, CNR, Pisa, Italy

<sup>1</sup> also at INFN-Pisa, Pisa, Italy

<sup>2</sup> also at CSFNSM, Catania, Italy

<sup>3</sup> also at INFN- Milano, Milano, Italy

## Abstract

This paper describes the activities carried out at the Laser-driven Light Ions Acceleration Line (L3IA) at the ILIL Lab in Pisa including the first radiobiological assay irradiation of multi-Gy, multi-MeV laser-driven proton beam at ultrahigh dose-rates.

## LASER-DRIVEN PROTON ACCELERATION APPLICATIONS (LPA2)

Novel ion acceleration techniques [1] based on ultra-intense lasers are evolving rapidly relying on established and extensively investigated acceleration processes like the Target Normal Sheath Acceleration (TNSA) [2]. In 2016, within the frame of a joint experiment between INFN and CNR, we started the construction of an advanced line for laser-driven light ions acceleration (L3IA) [3] which had the purpose of establishing an outstanding beam-line operation of a laser-plasma source in Italy.

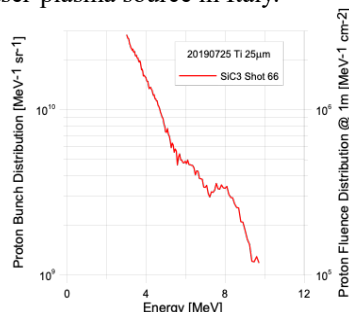


Figure 1: L3IA performance spectrum.

The beam-line operates at a newly developed sub-PW scale laser installation able to achieve the parameters range of ion acceleration currently explored by leading European laboratories [4] and was aimed to provide an advanced test facility for the development and exploitation of laser-driven ion sources. The spectrum reported in Fig.1 shows a typical measurement of the beamline performances measured at 1361 mm from the interaction point with a SiC detector at 1.4° with respect to the normal line to the target.

## The Laser System

The experiment was carried out at the Intense Laser Irradiation Laboratory (ILIL) [5] of the National Institute of

Optics of the Italian CNR, located in Pisa, Italy. In particular, the 220 TW beamline of the ILIL-PW Ti:Sa laser was used. During the experiment, up to 4J energy pulses were delivered on target, with pulse duration of 27 fs. The beam was focused on target by a f/4.5 off-axis parabolic (OAP) mirror in a 4.4 µm (FWHM) average diameter spot at an angle of incidence of 15°. The laser intensity on target was up to  $2.4 \times 10^{20} \text{ W/cm}^2$  ( $a_0=10.6$ ).

## The Target Holding System and Materials

As shown in Fig. 2, the target mount consisted of a couple of solid steel frames machined to leave access to the surface of the foil target (placed in the middle) from both sides through a set of 1000 µm diameter holes with conical 120° aperture to allow oblique laser incidence on target. These specifications ensure that the scanning of targets up to 100 mm × 100 mm can be accomplished (with a resolution/repeatability of the order of 1 µm), enabling a large number of laser shots (100) to be fired on a given target before target replacement is required. The system is fully remote controlled and driven in all the 3 main axes.

The solid target foils used in the experiment are made of aluminium, copper, molybdenum and titanium with thickness ranging from a few microns up to 30 µm. The material was of the annealed type and we finally chose to use light tight specification.

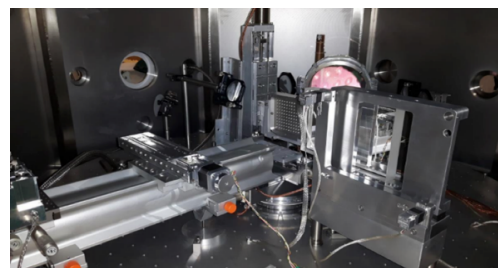


Figure 2: Target mount inside the vacuum chamber.

## The proton beam detectors

In order to characterise and monitor the light ions source in real time, a set of particle detectors have been developed.

For each laser shot, diagnostic tools measure not only the cut-off energy, but also the energy distribution of the accelerated proton bunch. Considering the short distance between the detector and target (0.3-1.5 m), for multi-MeV TNSA proton bunch very fast detectors and DAQ are required (GHz in bandwidth). We selected thin diamond and SiC planar diodes as the optimal choice. In particular, SiC Schottky diodes developed in the framework of the INFN SiCILIA experiment have been extensively used (10  $\mu\text{m}$  in thickness and areas of 2.5 and 20  $\text{mm}^2$ ).

The sensitivity of our ToF spectrometer is about  $10^9 \text{ MeV}^{-1}\text{sr}^{-1}$  and is limited by the residual EM noise in the interaction chamber.

### The Beam Formation and Transport

To support the radiobiology activities, we performed a dedicated set of measurements aimed to qualify in detail beam source parameters as cut-off energy, angular divergence and shot intensity looking at properties related to stability and reproducibility. At the same time, we carried out preliminary studies and developed a set of computing tools devoted to beam dynamics computations along the beam line. Beam dynamics studies were developed to refine a set of routines that would allow optimising the beam characteristics at the cell sample position. The Fig. 3 describes a configuration for the transport of the beam up to a distance of 1000 mm from the source using the 4 PMQs of the Elimed experiment [2]

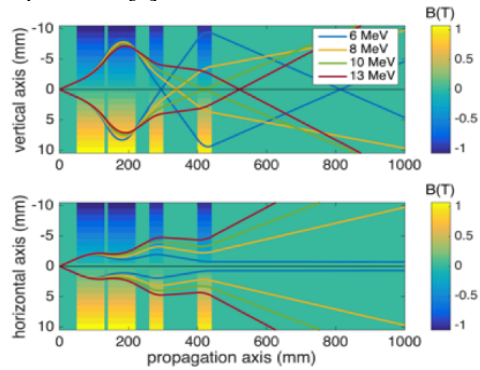


Figure 3: Modelling of the proton beam transport system.

This study has been considered of great importance in the definition of the cell's position. The laser experimental chamber extends up to 820 mm from the source, while the quads end at 433 mm. The cells must be positioned in air for practical reasons.

Considerations due to beam intensity along the beam path along with measured beam energy at different positions forced us to consider installing a reentrant window with a vacuum air interface at 453 mm from the beam source (position named P2). The energy distribution at this point is reported in Fig. 4.

## THE RADIobiology EXPERIMENT

### The Experimental Setup

A schematic view of the experimental setup is shown in Fig. 5. We use permanent magnet quadrupoles to select

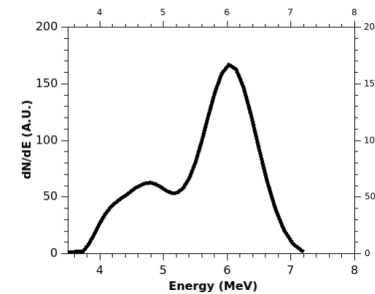


Figure 4: Typical proton spectrum downstream of the quadrupole beamline.

protons at 6 MeV and transport them, in the form of a collimated beam, to the final target position in air where the radiobiological sample is placed. We measured the delivered dose at the sample position for each shot, through radiochromic films, as well as the beam spectrum.

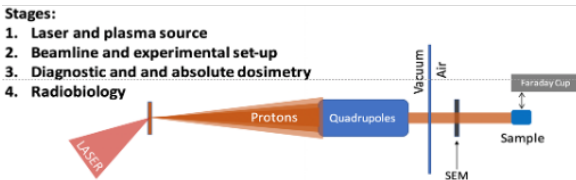


Figure 5: Schematic of the experimental set up.

### The Beam Characterization Process

The preliminary dosimetric beam characterization was carried out in terms of short-term reproducibility (i.e. shot-to-shot dose stability) and linearity with absorbed dose. The short-term reproducibility, calculated as the percentage ratio of the standard deviation to the mean RCF output in terms of PixelValue, was evaluated over five consecutive irradiations under the same experimental conditions. Five different stacks, each of them consisting of three previously calibrated RCFs (A, B and C), EBT3-Unlaminated type [6], were placed 2 mm behind the beam exit window and the dose evaluated in a selected ROI of maximum beam homogeneity (see Fig. 6).

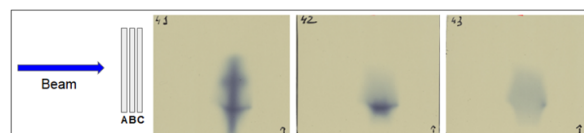


Figure 6: Example of one of the five irradiated RCF stacks.

The short-term reproducibility resulted to be smaller than 3.38%, 1.88% and 1.69% for the position A, B and C respectively, thus indicating a good stability of the laser system and its capability to be used for radiobiological experiments. The linearity over a dose range typically adopted in the proton therapy clinic, up to about 8 Gy, was also evaluated by irradiating five different calibrated RCFs, EBT3 type [7], with an incremental number of shots. A remarkable linear behaviour was observed, the dose increasing with the number of shots with a correlation fitting factor  $R > 0.99$ .

In order to provide on-line information on the released dose in each proton bunch for radiobiological irradiations,

a Secondary Emission Monitoring (SEM) system, consisting of a thin (12.5 mm-thick) tantalum foil electrically insulated by means of a PMMA circular frame able to detect the secondary electrons generated by the interaction of the protons with the detector itself and positioned in-air between the beam exit window and the cells irradiation point, was cross-calibrated against the RCFs. A calibration factor of  $(2.11 \pm 0.01) \times 10^8$  Gy/C, calculated by averaging the ratios between the RCF dose measurements and the collected charge by the SEM over a range of doses between 1.5 and 3.0 Gy, was thus estimated, allowing to convert the collected charge into absorbed dose in water and providing a real-time measurement of the delivered dose.

#### Biological Endpoint and Its Rationale

One biological endpoint selected for our study is the Cytokinesis-block micronucleus (CBMN) assay (see Fig. 7). Since the mid-1960s, the analysis of dicentric chromosomes in peripheral blood lymphocytes (PBLs) has been the gold standard for the measurement of radiation-induced biological effects and the dose assessment in the framework of radiological protection programmes [8]. Nowadays, the cytokinesis-block micronucleus (CBMN) assay is an alternative and routinely used method for the biological dosimetry of radiation [9,10]. The micronucleus (MN) assay is less complex and faster than the dicentric chromosome assay and permits to analyse a large number of cells in a relatively short time, thus increasing the statistical power of the assessment of damage.

MN are small extranuclear bodies found in the cytoplasm outside the main nucleus and contain acentric fragments or whole chromosomes that are not included in the daughter nuclei following DNA replication and mitosis [11,12]. MN are usually scored in PBLs, which have accomplished a mitosis due to the stimulation of phytohemagglutinin (PHA). These cells can be identified as binucleated (BN) cells by addition of the cytoplasmic division inhibitor cytochalasin B during cell culture.

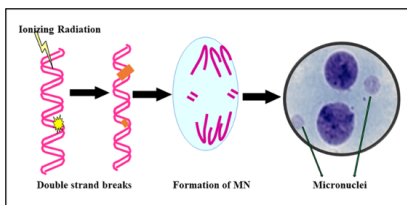


Figure 7: Schematic of the CBMN.

The standard procedure for CBMN assay requires the use of a minimum amount of blood (0.3–0.4 ml) to which is added as a mitogenic agent (PHA) in a culture medium to stimulate T-lymphocytes, which are the most appropriate system among blood cells for biological dosimetry. T-lymphocytes are extremely radiosensitive and offer many advantages over other cells in the study of radiation-induced chromosome damage and the relative biological effectiveness of different radiation types [8,9,13]. Indeed, T-lymphocytes in blood samples are all irradiated while they are synchronised in the G0 phase of the cell cycle, a quiescent state outside of the replication state [13,14]. After stimulation

by PHA, T-lymphocytes go into mitosis making it possible to uncover the effects of the radiation on the cell. Radiation-induced MN observed in PBL are the result of unrepaired or misrepaired double-strand breaks by the non-homologous end joining (NHEJ) repair pathway [12,13]. Radiation-induced MN clearly shows a dose-rate effect and depends on the radiation quality [15–18]. Therefore, the CBMN assay is a rigorously validated and standardised technique in the field of radiation biology and, hence, a very reliable method to gain insights into the biological effects of ultrahigh dose-rate.

## RESULTS AND DISCUSSION

Preliminary measurement of radiation damage vs dose based on the MN assay was successfully carried out. Blood samples from two different donors were used showing very similar results. A summary of the data is shown in Fig. 8 where the number of cells with micronuclei and the total number of micronuclei over thousand binucleated cells are shown for unirradiated cells and cells after irradiation with increasing number of shots. While further analysis is in progress we can anticipate that the dose per shot is approximately 1 Gy.

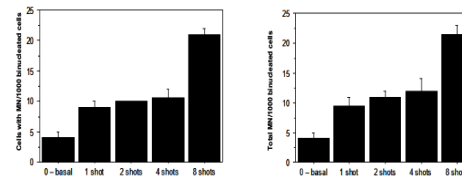


Figure 8: Number of cells with micronuclei (left) and total number of micronuclei (right) over thousand binucleated cells for increasing number of shots.

According to these measurements, the MN frequency increases with dose as expected. However, MN frequency is found to increase slowly for 1, 2 and 4 shots, while a significant increase is seen for 8 shots, suggesting threshold mechanism occurring between 4 and 8 shots. The full analysis of these results, including the unexpected behaviour with increasing dose is currently in progress.

## CONCLUSIONS AND PERSPECTIVES

Dosimetry at sample position for a laser-driven 6 MeV proton source was successfully carried out experimentally showing stable, reproducible and uniform irradiation at sample. First MN assay was successfully carried out on blood samples of two different donors with dose scaling up to 8 Gy, enabling a comparison between UHDR (single pulse) and dose averages over multiple shots.

## ACKNOWLEDGEMENTS

The activities described have been supported by INFN CSN5 National Committee. The research leading to these results has received funding from the CNR funded Italian research Network ELI-Italy (D.M. No. 631 08.08.2016), the EU funded Eupraxia PP (GA 101079773) and IFAST (GA 101004730).

## REFERENCES

[1] A. Macchi *et al.*, "Ion acceleration by superintense laser-plasma interaction", *Rev. Mod. Phys.*, vol. 85, pp. 751-793, May 2013. doi:10.1103/RevModPhys.85.751

[2] F. Schillaci *et al.*, "Characterization of the ELIMED Permanent Magnets Quadrupole system prototype with laser-driven proton beams", *J. Instrum.*, vol. 11, no. 7, p. T07005, Jul. 2016. doi:10.1088/1748-0221/11/07/T07005

[3] L.A.Gizzi *et al.*, "A New Line for Laser-Driven Light Ions Acceleration and Related TNSA Studies", *Appl. Sci.*, vol. 7, no. 10, p. 984, (2017. doi:10.3390/app7100984

[4] Laserlab Site, <https://www.laserlab-europe.eu/>

[5] L.A.Gizzi, *et al.*, "Overview and specifications of laser and target areas at the Intense Laser Irradiation Laboratory", *High Power Laser Sci. Eng.*, vol. 9, p. e10, 2021. doi:10.1017/hpl.2020.47

[6] Ashland – Unlaminated Films, <https://www.ashland.com/industries/medical/gafchromic-dosimetry-films/unlaminated-films>

[7] Gafchromic – EBT3 techniacal specifications, [http://www.gafchromic.com/documents/EBT3\\_Specifications.pdf](http://www.gafchromic.com/documents/EBT3_Specifications.pdf)

[8] IAEA, "Biological dosimetry: chromosomal aberration analysis for dose assessment", Vienna, Austria, Rep. Series No. 260, 1986.

[9] IAEA, "Cytogenetic analysis for radiation dose assessment", Vienna, Austria, Rep. Series No. 405, 2001.

[10] M. Fenech *et al.*, "Measurement of Micronuclei in lymphocytes", *Mutat Res.*, vol. 147, pp. 29-36, 1985. doi:10.1016/0165-1161(85)90015-9

[11] M. Fenech *et al.*, "The in vitro micronucleus technique", *Mutat. Res.*, vol. 455, pp. 81-95, 2000. doi:10.1016/s0027-5107(00)00065-8

[12] M. A. Bender *et al.*, "Dna Synthesis and Mitosis in Cultures of Human Peripheral Leukocytes", *Exp. Cell Res.*, vol. 27, pp. 221-229, 1962. doi:10.1016/0014-4827(62)90225-2

[13] H. Vral *et al.*, "Study of Dose-rate and Split-dose Effects on the in Vitro Micronucleus Yield in Human Lymphocytes Exposed to X-rays", *Int. J. Radiat. Biol.*, Vol. 61, no. 6, pp.777-784, 1992. doi:10.1080/09553009214551641

[14] J. Prosser, "The Cytokinesis-Block Micronucleus", *Mutat Res.*, vol. 199, p. 37, 1988.

[15] B. Sreedevi *et al.*, "Assay of Micronuclei in Peripheral Blood Lymphocytes as a Biological Indicator of Radiation Dose", *Radiat Prot Dosimetry*, vol. 51, pp. 41-45, Jan. 1994. doi:10.1093/oxfordjournals.rpd.a082120

[16] H. Thierens *et al.*, "Biological dosimetry using the micronucleus assay for lymphocytes: interindividual differences in dose response", *Health Phys.*, vol. 61, no. 5, pp.623–630, 1991.

[17] J. Miszczyk, "Response of human lymphocytes to proton radiation of 60 MeV compared to 250 kV X-rays by the cytokinesis-block micronucleus assay", *Radiother Oncol.*, vol. 115, pp. 128-134, 2015. doi:10.1016/j.radonc.2015.03.003

[18] S. Acharya, "Dose rate effect on micronuclei induction in human blood lymphocytes exposed to single pulse and multiple pulses of electrons", *Radiat Environ Biophys.*, vol. 50, pp. 253-263, 2011. doi:10.1007/s00411-011-0353-1